Egyptian Journal of Basic and Applied Sciences 5 (2018) 87–99

HOSTED BY

Contents lists available at ScienceDirect

Egyptian Journal of Basic and Applied Sciences

journal homepage: www.elsevier.com/locate/ejbas

Synthesis, characterization and anticancer activity of vincristine loaded folic acid-chitosan conjugated nanoparticles on NCI-H460 non-small cell lung cancer cell line

Naresh Kumar [a], Raj Kumar Salar [a,*], Minakshi Prasad [b], Koushlesh Ranjan [c]

[a] Department of Biotechnology, Chaudhary Devi Lal University, Sirsa 125055, Haryana, India
[b] Department of Animal Biotechnology, Lala Lajpat Rai University of Veterinary & Animal Sciences, Hisar 125001, Haryana, India
[c] Department of Veterinary Physiology and Biochemistry, Sardar Vallabhbhai Patel University of Agriculture, Meerut, 250110, Uttar Pradesh, India

ARTICLE INFO

Article history:
Received 14 August 2017
Received in revised form 31 October 2017
Accepted 15 November 2017
Available online 26 November 2017

Keywords:
Cancer
Chitosan
Vincristine

ABSTRACT

Vincristine is used to treat different type of cancers. But unwanted side effects limit their applications in medicine. To overcome these side effects by targeted drug delivery approach, we synthesized vincristine loaded folic acid-chitosan conjugated nanoparticles by ionic gelation method. The nanoparticles were characterized using Dynamic Light Scattering (DLS), Fourier Transform Infrared Spectroscopy (FTIR), Scanning Electron Microscopy (SEM) and Transmission Electron Microscopy. DLS confirmed small sized nanoparticles (<200 nm) while FTIR confirmed different functional groups associated with synthesized nanoparticles. SEM showed spherical shaped nanoparticles with smooth surface, whereas, TEM confirmed loading of vincristine in folic acid-chitosan conjugated nanoparticles. Anticancer activity of vincristine loaded folic acid-chitosan conjugated nanoparticles was checked by MTT assay on NCI-H460 cells followed by reactive oxygen species level, mitochondrial transmembrane potential and apoptotic morphological changes, which confirmed the cytotoxicity of nanoparticles. Erythrocyte aggregation assay confirmed non-toxicity of nanoparticles. Hence, these nanoparticles can be used to treat NCI-H460 cells.

1. Introduction

Non-small cell lung cancer (NSCLC) is major type of lung cancer that bears almost 85% of major lung cancer types. Only 17.3% of the people who develop NSCLC survive for 5 years. NSCLC is an aggressive neoplasm, responsible for more lung cancer related deaths every year in the United States than colon, breast, pancreas, and prostate cancers combined together [1]. The major types of NSCLC are – adenocarcinoma (nearly 40%), squamous cell carcinoma (nearly 25–30%) and large cell carcinoma (nearly 10–15%) [2]. Chemotherapy, radiotherapy and surgery have been used to treat NSCLC but have serious side effects. Vincristine is used in clinical practice since the early 1960s [3,4]. Vincristine is used to treat different types of cancers, which include acute lymphocytic leukemia, acute myeloid leukemia, Hodgkin's disease, neuroblastoma and lung cancer [5]. It is a vinca alkaloid and obtained from the Madagascar periwinkle *Catharanthus roseus* [6]. However, multidrug resistance, unwanted side effects on healthy cells and poor availability to cancer cells limit its utilization in medicine. In a few years, anticancer drugs loaded natural and artificial polymers have been tested against cancer cell lines to bypass the p-glycoprotein receptors, the main cause of drug resistance.

Among different polymers, chitosan, the cationic polysaccharide, has drawn attention in pharmaceutical and biomedical applications due to its bioavailability, mucoadhesivity, biocompatibility, biodegradability, non-toxicity and low-immunogenicity [7–9]. Chitosan is composed of (1 → 4) linked D-glucosamine and N-acetyl-D-glucosamine units obtained by deacetylation of chitin, which is a natural polysaccharide present in the exoskeleton of crustaceans such as crabs and shrimps [7]. Chitosan is thought to be degraded in vertebrates by lysozyme and bacterial enzymes in the colon [10]. These properties make chitosan as an excellent carrier for anticancer drugs. Chitosan nanoparticles can be made target specific to tumor by attaching ligands. The incorporation of targeting ligands with chitosan does not change its physicochemical and biochemical properties [11,12]. When compared to other targeting ligands, folic acid is less expensive, can be conjugated to drug delivery carriers easily, and more stable in processing, storage and applications [13]. In this study, vincristine loaded folic acid-chitosan conjugated nanoparticles were synthesized, characterized by different techniques and anticancer activity of nanoparticles was checked against NCI-H460 non-small cell lung cancer cell line.

* Corresponding author.
E-mail addresses: rajsalar@rediffmail.com, rajsalar@cdlu.in (R.K. Salar).

https://doi.org/10.1016/j.ejbas.2017.11.002
2314-808X/

2. Materials and methods

2.1. Chemicals

Low molecular weight chitosan (≥75% deacetylation degree), N-hydroxysuccinimide (NHS), N,N′-dicyclohexylcarbodiimide (DCC), dimethyl sulfoxide (DMSO), triethylamine, sodium acetate, sodium hydroxide, sodium tripolyphosphate (85%), acetic acid, folic acid, Hoechst 33258, 3-(4,5-dimethylthiazol-2-yl)-2,5-diphenyl tetrazolium bromide (MTT), 2′-7′ dichlorodihydrofluorescein diacetate (DCFH-DA), rhodamine 123 (Rh-123), acridine orange (AO), ethidium bromide (EtBr) were purchased from Sigma Aldrich. Phosphate buffered saline (Dulbecco A), Acetate buffer (pH 5.6) and RPMI-1640 medium were purchased from HiMedia Laboratories, India. All the chemicals were of analytical grade. Non-small cell lung cancer cell line (NCI-H460) was purchased from National Centre for Cell Science (NCCS), Pune, India.

2.2. Synthesis of N-hydroxysuccinimide-ester of folic acid

N-hydroxysuccinimide-ester of folic acid was synthesized according to the previously reported method [14]. Prepared 1 M solution of N-hydroxysuccinimide and N,N′-dicyclohexylcarbodii mide. An amount of 1.5 g of folic acid was dissolved in 25 ml of dimethyl sulfoxide (DMSO) and added 2 ml of 1 M N-hydroxysuccinimide (NHS) and N,N′-dicyclohexylcarbodiimide (DCC). To this solution, added 2 ml of triethylamine and allowed the reaction to proceed for 17 h under stirring in the dark. Pale yellow colored dicyclohexylurea was removed through filter paper of 125 μm pore size and washed yellow N-hydroxysuccinimide-ester with 30% acetone solution.

2.3. Synthesis of folic acid-chitosan (FA-CS) conjugate

An amount of 45 mg of chitosan was dissolved in 15 ml of acetate buffer (pH 5.6) in a flask with magnetic stirring for a few minutes. Took 200 mg of N-hydroxysuccinimide-ester of folic acid and dissolved in 15 ml of DMSO. Added solution of N-hydroxysuccinimide-ester of folic acid in chitosan solution drop wise for synthesis of folic acid-chitosan conjugate. The mixture was stirred at 30 °C in the dark for 20 h.

2.4. Synthesis of blank and vincristine loaded folic acid-chitosan conjugated (FA–CS) nanoparticles

Blank and vincristine loaded folic acid-chitosan conjugated (FA–CS) nanoparticles were synthesized by ionic gelation method with slight modifications [15]. A stock solution of acetic acid (2%, v/v) and FA-CS solution (0.2%, w/v) was prepared by dissolving 0.2 g of FA-CS conjugate in 100 ml of acetic acid (2%, v/v). The pH of FA-CS solution was adjusted to 5 with 1 N NaOH and HCl. A stock solution of sodium tripolyphosphate (TPP) (0.5%, w/v) was prepared by dissolving 250 mg in 50 ml double distilled water. Also prepared a stock solution of vincristine in water (1 mg/10 ml, pH 4.77). For synthesis of blank folic acid-chitosan conjugated nanoparticles, added 25 ml of folic acid-chitosan conjugate solution in a flask and then added 5 ml sodium tripolyphosphate to it drop wise to make 1:5 ratio till the formation of nanoparticles suspension and allowed to stir for 30 minutes on a magnetic stirrer at room temperature. For the synthesis of vincristine loaded nanoparticles, took constant volume (25 ml) of folic acid-chitosan conjugate predissolved in acetic acid in four separate flasks, added varying volumes of stock solutions of vincristine (100 μl, 200 μl, 300 μl, 400 μl) in these flasks and then added sodium tripolyphosphate (5 ml) in each flask drop wise. The solution was allowed to stir for 30 minutes on a magnetic stirrer at room temperature. The synthesized vincristine loaded folic acid-chitosan conjugated nanoparticles were labeled as 1:25, 2:25, 3:25 and 4:25 formulations, respectively. Nanoparticles suspension of blank and vincristine loaded folic acid-chitosan conjugated nanoparticles was centrifuged at 16,000 rpm for 30 minutes to separate nanoparticles from solution for further characterization.

2.5. Characterization

2.5.1. Average size, polydispersity index and zeta potential

Average size, polydispersity index and zeta potential of nanoparticles were measured by dynamic light scattering (DLS) using Malvern Zetasizer Nanos ZS90 (Malvern Instruments, UK). The nanoparticles (50 μl) were dispersed in double distilled water (950 μl) to make 1 ml solution and readings were taken at 25 °C. Three different batches were analyzed to give an average value and standard deviation for the average size, polydispersity index and zeta potential.

2.5.2. Encapsulation efficiency (%) and loading capacity (%)

The encapsulation efficiency (%) and loading capacity (%) of vincristine loaded folic acid-chitosan conjugated nanoparticles were determined by centrifuging samples at 16,000 rpm for 30 minutes. The contents of free vincristine in the supernatant was determined by UV spectrophotometer (NanoDrop 2000c, Thermo Scientific, Wilmington, DE, USA) at 220 nm wavelength using supernatant of their corresponding blank nanoparticles as basic correction. The encapsulation efficiency (%) and loading capacity (%) were calculated by following equations:

$$\text{Encapsulation efficiency } (\%) = (\text{Vincristine})_{\text{tot}} - (\text{Vincristine})_{\text{free}}/(\text{Vincristine})_{\text{tot}} \times 100 \quad (1)$$

$$\text{Loading capacity } (\%\ \text{w/w}) = \text{Mass of vincristine in chitosan nanoparticles} / \text{Mass of chitosan nanoparticles recovered} \times 100 \quad (2)$$

2.5.3. Storage stability of nanoparticles

Storage stability of blank and vincristine loaded folic acid-chitosan conjugated nanoparticles was measured in sodium phosphate buffer (pH 7.4) at 4 °C in a refrigerator. The average size, polydispersity index and zeta potential were measured with dynamic light scattering (DLS) after 10 days using Malvern Zetasizer Nanos ZS90 (Malvern Instruments, UK). The nanoparticles (50 μl) were dispersed in double distilled water (950 μl) to make 1 ml solution and readings were taken at 25 °C. Experiment was performed in triplicates. Average value and standard deviation for the average size, polydispersity index and zeta potential were measured.

2.5.4. Fourier transform infrared spectroscopy (FTIR)

The Fourier transform infrared (FTIR) spectra of blank and vincristine loaded chitosan nanoparticles were analyzed by Spectrum RX-IFTIR spectrometer (PerkinElmer, Waltham, MA, USA). Dried nanoparticles were mixed with potassium bromide (KBr) in 2% w/w ratio. The mixture was ground into fine powder and compressed into potassium bromide disc under a hydraulic press at 10,000 psi. Each potassium bromide disc was scanned over a wave number region from 4000 cm^{-1} to 400 cm^{-1} with resolution of 1 cm^{-1}. Characteristic peaks of functional groups for different samples were recorded.

2.5.5. Scanning electron microscopy (SEM)

The morphology of blank and vincristine loaded chitosan nanoparticles were analyzed by scanning electron microscope

(JEOL Model JSM – 6390LV). For this, a small quantity of samples were placed in aluminum stubs and then coated with platinum. The SEM images were taken under accelerated electrons with voltage of 15 kV.

2.5.6. Transmission electron microscopy (TEM)

Loading of vincristine in folic acid-chitosan conjugated nanoparticles was examined by transmission electron microscope (Jeol/JEM 2100, Peabody, MA, USA). A drop of nanoparticles was dried on copper grid and TEM images were taken at operating voltage of 200 kV.

2.5.7. In vitro release study

In vitro release study of vincristine loaded folic acid-chitosan conjugated nanoparticles were analyzed by dialysis tubing (molecular weight cut off between 12,000–14,000 Da) in phosphate buffered saline (pH 6.7) at 37 °C [14]. Vincristine loaded nanoparticles (10 mg) were dispersed in 1 ml of phosphate buffered saline and placed in dialysis tube. This tube was immersed in 50 ml phosphate buffered saline and shaken at 105 rpm at 37 °C. At definite interval of time, release media were collected and replaced with fresh phosphate buffered saline. The concentration of the released vincristine into phosphate buffered saline was determined at 220 nm wavelength with UV–Vis spectrophotometer (NanoDrop 2000c, Thermo Scientific, Wilmington, DE, USA).

2.5.8. Analysis of vincristine uptake by fluorescence microscopy

The cellular uptake of vincristine loaded folic acid-chitosan conjugated nanoparticles in NCI-H460 cells was analyzed by fluorescence microscopy. Cells were incubated with 100 μl of Hoechst 33258 dye (0.5 μg/ml, blue fluorescence) at 37 °C for 1 h in a CO_2 incubator and washed twice with PBS (pH 7.4) by centrifuging at 5000 rpm for 5 minutes (Velocity 18 R, Refrigerated centrifuge, Dynamica, United Kingdom). The washed cells were resuspended in RPMI-1640 medium and incubated with 100 μl of vincristine loaded folic acid-chitosan conjugated nanoparticles (10 mg/ml, 4:25 formulation) at 37 °C for 45 minutes. Cells were then examined under a fluorescence microscope using blue fluorescence at 40× magnification (Nikon TiS Eclipse fluorescence Microscope, Tokyo, Japan).

2.5.9. Anticancer activity of vincristine loaded folic acid-chitosan conjugated nanoparticles

2.5.9.1. Cell culture. The research work on non-small cell lung cancer cell line (NCI-H460) was carried out at Department of Animal Biotechnology, Lala Lajpat Rai University of Veterinary and Animal Sciences, Hisar. NCI-H460 cells were purchased from National Centre for Cell Science (NCCS), Pune, India. Cells were cultured as a monolayer on RPMI-1640 medium supplemented with 1 mM sodium pyruvate, 2 mM L-Glutamine, 4.5 g glucose per litre and 1.5 g per litre sodium bicarbonate without HEPES buffer, 10% fetal bovine serum (FBS), penicillin and streptomycin in a humidified atmosphere of 95% air and 5% CO_2 at 37 °C. Cells were grown in 75 cm^2 tissue culture flasks and used for experiments when in exponential growth phase.

2.5.9.2. MTT assay. The cytotoxicity of vincristine loaded folic acid-chitosan conjugated nanoparticles was determined by method of Mosmann [16] with slight modifications. The cells (1 ml, 1×10^6 cells/ml) were cultured in a 96 well plate and treated with different concentrations of blank and vincristine loaded folic acid-chitosan conjugated nanoparticles (5, 10, 15, 20 and 25 mg/ml dissolved in phosphate buffered saline) of 4:25 formulation. The cells were incubated with 95% air and 5% CO_2 at 37 °C for 16 h in a CO_2 incubator. Cells in PBS (pH 7.4) with RPMI-1640 medium and RPMI-1640 medium alone were used as negative control. Added 10 μl stock MTT dye solution (5 mg/ml) to each well and incubated the plate at 37 °C for 2 h. The medium was removed with the help of a micropipette carefully without disrupting the cells and added 100 μl of anhydrous isopropanol (0.1 N HCl) in each well. The cells were incubated at 37 °C for 2 h with 95% air and 5% CO_2 at 37 °C. Spectrophotometric readings of each well were taken at 570 nm with Synergy 2 Multi-Mode Reader (BioTek, Winooski, VT, US). IC_{50} values were calculated and the optimum dose was used for further study. The percent cell viability was calculated by following equation:

$$\text{Cell viability}(\%) = \text{O.D. of cells treated with nanoparticles} / \text{O.D. of control cells} \times 100 \quad (3)$$

The NCI-H460 cells were divided into four experimental groups. Group 1: untreated control cells in RPMI-1640 medium, Group 2: untreated control cells in PBS (pH 7.4) with RPMI-1640 medium, Group 3: blank folic acid-chitosan conjugated nanoparticles (10 mg/ml), Group 4: vincristine loaded folic acid-chitosan conjugated nanoparticles (5 mg/ml).

2.5.9.3. Determination of intracellular reactive oxygen species (ROS) level. The intracellular ROS level was measured using a non-fluorescent probe, 2′,7′-dichlorofluorescin diacetate (DCFH-DA), which is oxidized by ROS to fluorescent dichlorofluorescein (DCF) in the living cells [17]. The NCI-H460 cells (1 ml, 1×10^6 cells/ml) were cultured in a 96 well plate with 95% air and 5% CO_2 at 37 °C in a CO_2 incubator. Cells were treated with blank (50 μl, 10 mg/ml in PBS) and vincristine loaded folic acid-chitosan conjugated nanoparticles (50 μl, 5 mg/ml in PBS). Untreated cells in RPMI-1640 medium and PBS (pH 7.4 + cells + RPMI-1640 medium) were used as negative control. The cells were incubated with 95% air and 5% CO_2 at 37 °C for 16 h. Added 50 μl of 10 μM 2′,7′-dichlorofluorescin diacetate stock solution prepared in DMSO, to each well and allowed to incubate at 37 °C for 30 minutes in a CO_2 incubator. The cells were washed with RPMI-1640 medium and observed under blue fluorescence using a fluorescence microscope (Nikon TiS Eclipse, Tokyo, Japan).

2.5.9.4. Determination of changes in mitochondrial transmembrane potential. The changes in mitochondrial transmembrane membrane potential in NCI-H460 cells treated with blank and vincristine loaded folic acid-chitosan conjugated nanoparticles were analyzed using Rhodamine-123 staining with slight modifications [17]. The NCI-H460 cells (1 ml, 1×10^6 cells/ml) were cultured in a 96 well plate with 95% air and 5% CO_2 at 37 °C in a CO_2 incubator, and then treated with blank (50 μl, 10 mg/ml in PBS) and vincristine loaded folic acid-chitosan conjugated nanoparticles (50 μl, 5 mg/ml in PBS). Cells with RPMI-1640 medium and PBS (pH 7.4 + cells + RPMI-1640 medium) were used as negative control and incubated at 37 °C for 16 h. Prepared a stock solution of Rhodamine (5 mmol/L) and added 50 μl in each well followed by incubation for 30 minutes in a CO_2 incubator. Cells were washed with RPMI-1640 medium and observed under blue fluorescence using a fluorescence microscope (Nikon TiS Eclipse, Tokyo, Japan).

2.5.9.5. Determination of apoptotic morphological changes. Acridine orange (AO) and ethidium bromide (EtBr) dual staining method was adopted to differentiate condensed apoptotic nuclei from normal cells [17]. The NCI-H460 cells (1 ml, 1×10^6 cells/ml) were cultured in a 96 well plate with 95% air and 5% CO_2 at 37 °C in CO_2 incubator. Cells were treated with blank (50 μl, 10 mg/ml in PBS) and vincristine loaded folic acid-chitosan conjugated nanoparticles (50 μl, 5 mg/ml in PBS). Cells with RPMI-1640 medium and PBS (pH 7.4 + cells + RPMI-1640 medium) were used as negative control and incubated at 37 °C for 16 h. Prepared stock solutions of acri-

dine orange and ethidium bromide (1 mg/ml) in PBS (pH 7.4). Cells were incubated with 5 μl each of acridine orange and ethidium bromide in each well at 37 °C for 30 minutes. Cells were washed with RPMI-1640 medium and observed under blue fluorescence using a fluorescence microscope (Nikon TiS Eclipse, Tokyo, Japan).

2.5.9.6. Erythrocyte aggregation assay. Aggregation assay was performed to check the toxic effect of nanoparticles on erythrocytes [17]. Since encapsulation efficiency (%) and loading capacity (%) of 4:25 formulation was maximum, hence selected for assay. Human blood was collected in a sterile tube containing ethylenediaminetetraacetic acid (EDTA). About 500 μl blood was centrifuged at 2000 rpm for 30 minutes to separate erythrocytes. Cells were washed with phosphate buffered saline (PBS, pH 7.4) twice and stored in the same buffer. To check the toxic effect of vincristine loaded folic acid-chitosan conjugated nanoparticles, 100 μl of erythrocytes were treated with 400 μl of nanoparticles dissolved in phosphate buffered saline (pH 7.4) and incubated for 1 h at 37 °C. Erythrocytes were observed at 40× magnification under a compound microscope (Magnus Analytics, New Delhi).

3. Results and discussion

3.1. Synthesis of N-hydroxysuccinimide ester of folic acid and folic acid–chitosan conjugate

Folic acid on reaction with N-hydroxysuccinimide (NHS), N,N′-dicyclohexylcarbodiimide (DCC) and triethylamine resulted in the formation of dark pale yellow colored dicyclohexylurea, confirming the synthesis of N-hydroxysuccinimide-ester of folic acid. Earlier, Salar and Kumar [14] observed yellow colored dicyclohexylurea while synthesizing vincristine loaded folic acid-chitosan conjugated nanoparticles at pH 2.5. Similarly, Ji et al. [18] also observed N-hydroxysuccinimide ester of folic acid during preparation of methotrexate loaded folic acid conjugated O-carboxymethyl chitosan nanoparticles. Further, folic acid-chitosan conjugate, dissolved in acetate buffer (pH 5.6) reacted with N-hydroxysuccinimide-ester of folic acid to form folic acid-chitosan conjugate. Similarly, Wang et al. [19] synthesized folic acid-chitosan conjugate, while loading mitoxantrone into folic acid-chitosan conjugated nanoparticles. Naghibi Beidokhti et al. [20] synthesized folic acid-chitosan conjugate by reaction of N-hydroxysuccinimide ester of folic acid with chitosan.

3.2. Blank and vincristine loaded folic acid-chitosan conjugated nanoparticles

The folic acid-chitosan conjugated nanoparticles were formed due to the ionic interaction between positively charged amino group ($-NH_3^+$) of the folic acid-chitosan conjugate and negatively charged sodium tripolyphosphate [18]. Folic acid-chitosan dissolved in acetic acid on reaction with sodium tripolyphosphate and different concentrations of vincristine, resulted in the formation of vincristine loaded folic acid-chitosan conjugated nanoparticles in different formulations. In earlier reports, Methotrexate loaded chitosan nanoparticles have been prepared by the ionic gelation method and tested against LNCaP prostate cancer cell line *in vitro* [21].

3.3. Characterization

3.3.1. Average size, polydispersity index and zeta potential

Average size of blank folic acid-chitosan conjugated nanoparticles was found to be 95.59 ± 0.52 nm with polydispersity index of 0.229 ± 0.31 and zeta potential of +8.91 ± 0.36 mV (Table 1). When vincristine was loaded in nanoparticles, a concentration dependant increase in the average size (nm) and zeta potential (mV) observed from 1:25 to 4:25 formulations. For formulation with maximum quantity of vincristine (4:25), average size of vincristine loaded folic acid-chitosan conjugated nanoparticles was 130.0 ± 0.89 nm with polydispersity index of 0.221 ± 0.01 and zeta potential of +9.83 ± 1.41 mV (Fig. 1). It has been reported that due to enhanced permeability effect, nanoparticles with size smaller than 200 nm can generally increase accumulation of anticancer drug in tumor [22]. Moreover, nanoparticles less than 200 nm have significantly longer circulation time because of low uptake by the reticuloendothelial system [23]. Vincristine loaded folic acid-chitosan conjugated nanoparticles in all formulations were below 200 nm in size, hence can be used for delivery against cancer cells. The positive zeta potential of all formulations favors uptake of nanoparticles by negatively charged cancer cells. In previous study, Salar and Kumar [14] observed large values of average size, polydispersity index and zeta potential of vincristine loaded folic acid – chitosan conjugated nanoparticles at pH 2.5 for same formulations. This showed that the pH of folic acid-chitosan conjugate solution dissolved in acetic acid prior to synthesis of nanoparticles has a controlling effect on average size, polydispersity index and zeta potential.

3.3.2. Encapsulation efficiency (%) and loading capacity (%)

Encapsulation efficiency (%) and loading capacity (%) of all formulations is shown in Table 2. A concentration dependant increase in the encapsulation efficiency (%) and loading capacity (%) of vincristine loaded folic acid-chitosan conjugated nanoparticles was observed with maximum for 4:25 formulation i.e. 95 ± 0.35 and 48.65 ± 0.47, respectively. These efficiencies were found higher as compared to vincristine loaded folic acid-chitosan conjugated nanoparticles synthesized at pH 2.5 by Salar and Kumar [14]. This showed that pH has effect on controlling the encapsulation efficiency (%) and loading capacity (%) of carrier system for anticancer drug. Earlier, Sun et al. [24] synthesized 5-fluorouracil loaded chitosan nanoparticles and observed maximum encapsulation efficiency and loading capacity of 44.28 ± 1.69% and 20.13 ± 0.007%, respectively when mass ratio of 5-fluorouracil and chitosan was 1:1. Xu et al. [25] reported encapsulation efficiency (85.4 ± 4.9%) and loading capacity (3.91 ± 0.12%) of gemcitabine in folic acid-chitosan conjugated nanoparticles.

3.3.3. Storage stability of nanoparticles

As shown in Table 3, there was increase in average size for all formulations after 10 days stored in sodium phosphate buffer (pH 7.4) and found maximum for 2:25 formulation i.e. 341.1 ± 0.58 nm. An increase in the polydispersity index was also observed, except 1:25 formulation. However, a decrease in the zeta potential was found in all formulations, except 3:25, but still was positive. Overall, there were variations in average size, polydispersity index and zeta potential, but was not significant. So it can be concluded that sodium phosphate buffer (pH 7.4) was suitable medium for storage of blank and vincristine loaded folic acid-chitosan conju-

Table 1
Average size, polydispersity index and zeta potential of vincristine loaded folic acid-chitosan conjugated nanoparticles at pH 5.

Formulations	Average size (nm)	Polydispersity index	Zeta potential (mV)
Blank FA-CS NPs	95.59 ± 0.52	0.229 ± 0.31	+8.91 ± 0.36
1:25	121.9 ± 0.95	0.271 ± 0.76	+9.11 ± 0.29
2:25	129.8 ± 0.30	0.250 ± 0.02	+9.38 ± 0.61
3:25	124.9 ± 0.96	0.249 ± 0.02	+8.96 ± 0.50
4:25	130.0 ± 0.89	0.221 ± 0.01	+9.83 ± 1.41

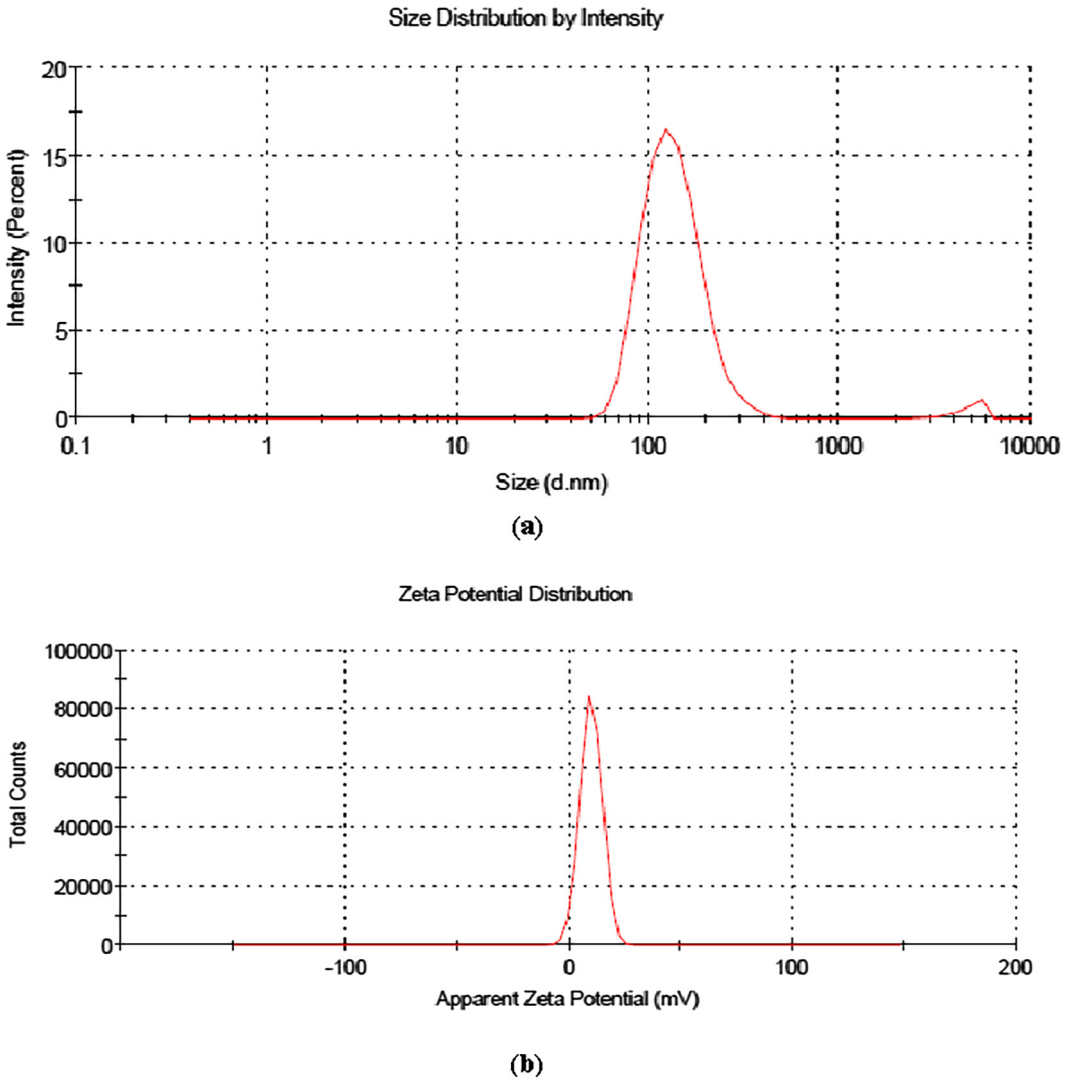

Fig. 1. Vincristine loaded folic acid-chitosan conjugated nanoparticles of 4:25 formulation (a) average size and polydispersity index, and, (b) and zeta potential.

Table 2
Encapsulation efficiency (%) and loading capacity (%) of vincristine loaded folic acid-chitosan conjugated nanoparticles.

S. No.	Formulations	Encapsulation efficiency (%)	Loading capacity (%)
1.	1:25	50 ± 0.58	10.90 ± 0.45
2.	2:25	70 ± 0.50	12.24 ± 0.51
3.	3:25	80 ± 0.45	25.40 ± 0.38
4.	4:25	95 ± 0.35	48.65 ± 0.47

± Standard deviation (n = 3).

Table 3
Effect of storage on average size, polydispersity index and zeta potential of blank and vincristine loaded folic acid-chitosan conjugated nanoparticles in sodium phosphate buffer (pH 7.4) at 4 °C after 10 days.

Formulations	After 10 days		
	Average size (nm)	Polydispersity index	Zeta potential (mV)
Blank FA-CS NPs	203.0 ± 0.50	0.329 ± 0.10	+3.94 ± 0.25
1:25	220.0 ± 0.96	0.259 ± 0.45	+2.76 ± 0.35
2:25	341.1 ± 0.58	0.611 ± 0.09	+3.74 ± 0.40
3:25	225.3 ± 0.34	0.547 ± 0.04	+4.25 ± 0.80
4:25	208.2 ± 0.43	0.336 ± 0.03	+3.83 ± 0.28

± Standard deviation (n = 3).

gated nanoparticles. An increase in the size of chitosan/tripolyphosphate nanoparticles stored in a phosphate buffer (pH 7.4) at 25 °C over a period of 10 days has been observed [26].

3.3.4. Fourier Transform Infrared Spectroscopy

The FTIR spectrum of blank folic acid-chitosan conjugated nanoparticles showed a characteristic peak at 3338.52 cm^{-1} due to N-H stretching vibration, which was shifted to 3336.79, 3326.54, 3355.91 and 3709.102 cm^{-1} for 1:25, 2:25, 3:25 and 4:25 formulations, respectively (Fig. 2a–e). Wider peak at 3709.102 cm^{-1} demonstrated that inter- and intra-molecular interactions were enhanced in folic acid-chitosan nanoparticles because of tripolyphosphoric groups of sodium tripolyphosphate linked with ammonium group of folic acid-chitosan conjugate [27]. Shifting in peaks at 1549.82, 1549.61, 1552.93 and 1551.94 cm^{-1} due to Amide II N-H deformation and C-N stretching vibration could be a consequence of loading of vincristine in nanoparticles.

3.3.5. Scanning electron microscopy (SEM)

Different sized nanoparticles with spherical shape and rough surface were observed by scanning electron microscopy (Fig. 3). However, there were difference in the size of nanoparticles as compared with dynamic light scattering (DLS) due to different tech-

niques used for preparation of nanoparticles for analysis. The nanoparticles in 4:25 formulation looked more rough in appearance, which might be due to maximum loading of vincristine in these. In contrast, Panwar et al. [28] observed smooth and spherical shaped ferulic acid-loaded chitosan nanoparticles and checked anticancer activity against ME-180 human cervical cancer cell lines. They observed significant inhibition in ME-180 cells and concluded that these nanoparticles can be used to treat cervical cancer. Anitha et al. [29] also observed spherical morphology of curcumin-loaded N,O-carboxymethyl chitosan nanoparticles and checked anticancer activity against normal (L929) and breast cancer cell line (MCF-7). The authors reported non-toxicity of nanoparticles against L929 cells, whereas enhanced toxicity was found against MCF-7 cells. In another report, Mehrotra et al. [30]

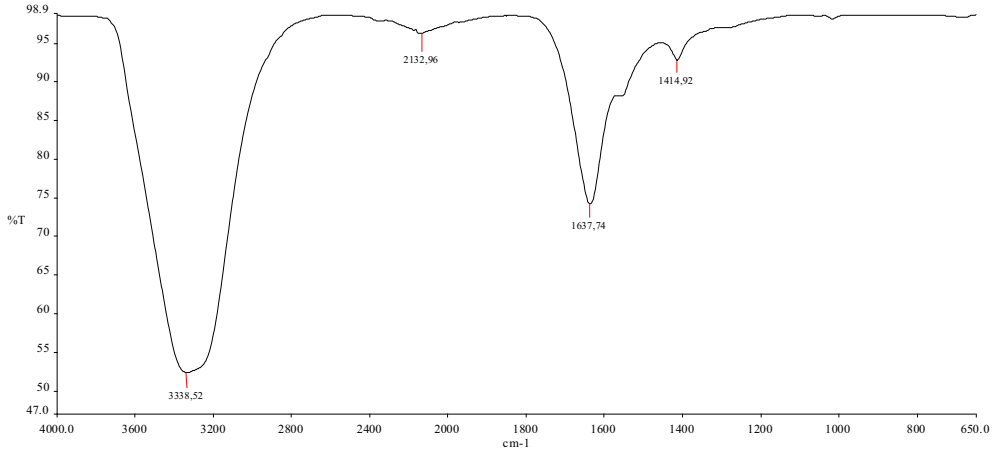

(a)

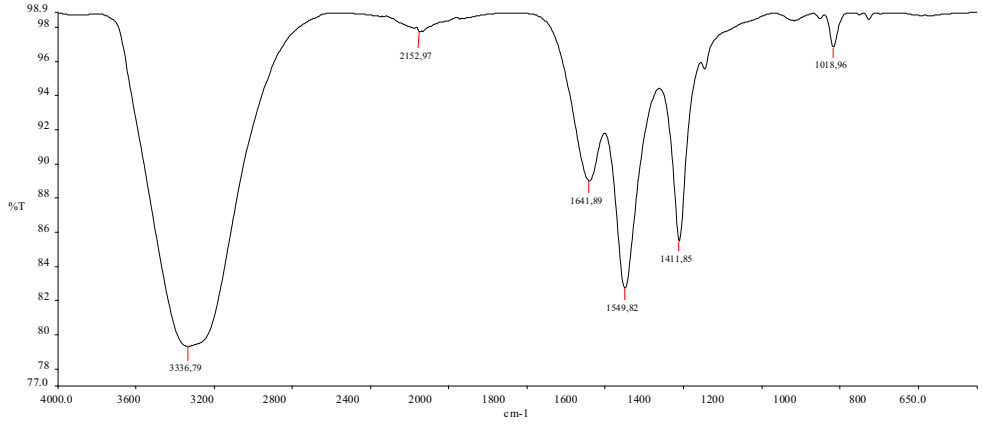

(b)

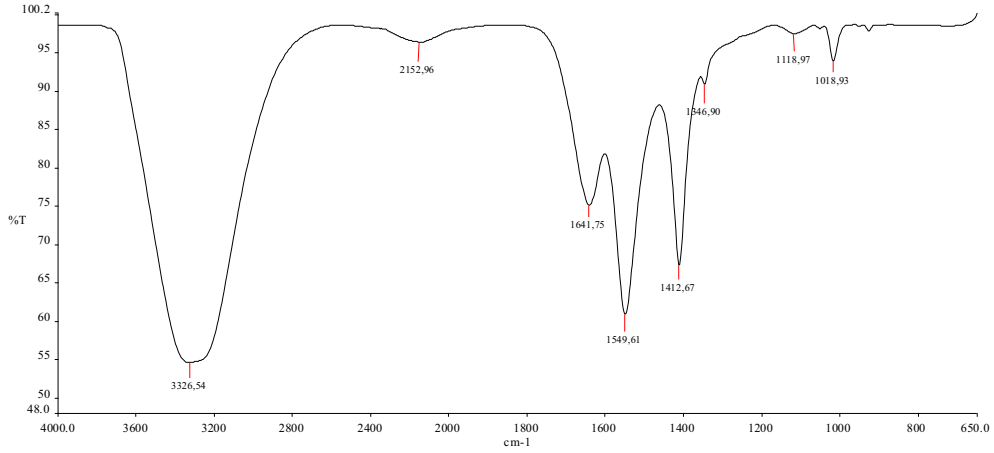

(c)

Fig. 2. FTIR spectra showing shifting in peaks due to loading of vincristine (a) blank FA-CS NPs and vincristine loaded FA-CS NPs at different formulations, (b) 1:25, (c) 2:25, (d) 3:25, (e) 4:25

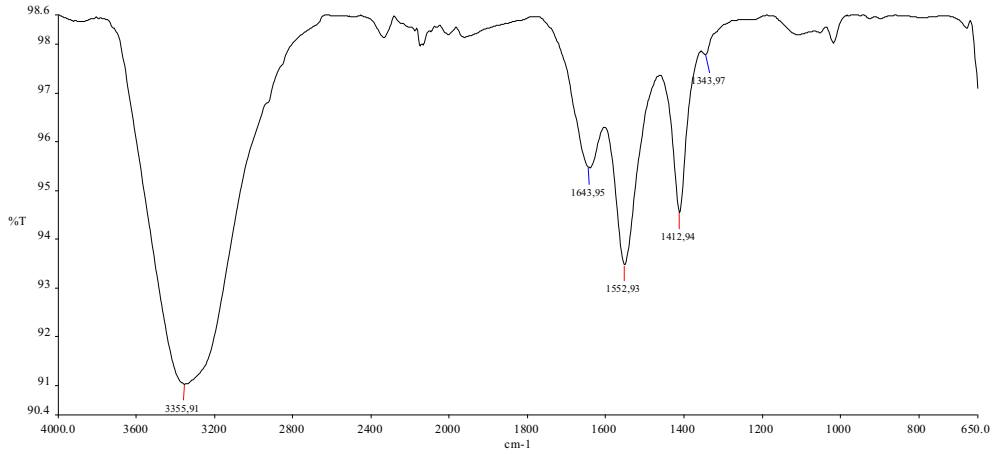

(d)

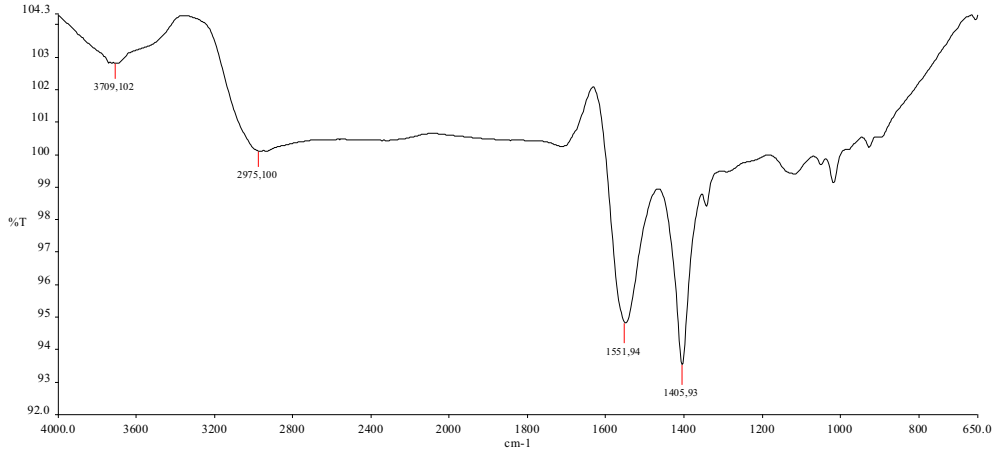

(e)

Fig. 2 (*continued*)

observed spherical shaped and smooth surfaced lomustine loaded chitosan sodium tripolyphosphate and chitosan-sodium hexametaphosphate nanoparticles.

3.3.6. Transmission electron microscopy (TEM)

As shown in Fig. 4, blank and vincristine loaded FA-CS nanoparticles were spherical in shape. As compared to blank FA-CS nanoparticles, granule like structures were present in nanoparticles of 1:25, 2:25, 3:25 and 4:25 formulations due to loading of vincristine. However, there were difference in the size of nanoparticles as compared with SEM due to more dilutions of sample used for preparation of nanoparticles for analysis in TEM. Earlier, Salar and Kumar [14] observed spherical shaped vincristine loaded folic acid-chitosan conjugated nanoparticles with granule like structure due to loading of vincristine. Similarly, spherical shaped mitoxantrone loaded folic acid-chitosan conjugated nanoparticles has also been observed [19].

3.3.7. In vitro release study

As shown in Fig. 5, 1:25 formulation showed 16.67% cumulative release of vincristine within 2 h and subsequently 16.71, 33.33 and 33.37% after 4, 6 and 8 h, respectively. As compared to this, 2:25 formulation showed 16.31% release within 2 h and 16.67, 16.71, 27.33% release after 4, 6 and 8 h, respectively. Similarly, a formulation of 3:25 showed 6.25% release within 2 h and after 4, 6, 8 h release was 6.07, 6.09, 12.5%, respectively. Finally, 4:25 formulation showed 5.51% release of vincristine within 2 h and subsequent release was 5.47, 5.57, 11.11% after 4, 6, 8 h, respectively from folic acid-chitosan conjugated nanoparticles. It can be concluded that, except 1:25, all formulations showed slow and sustained release of vincristine. Similarly, Wang et al. [19] observed slow release of mitoxantrone loaded in folic acid-chitosan conjugated nanoparticles in artificial gastric liquid (pH 1.2) and intestinal fluid (pH 6.8).

3.3.8. Uptake of vincristine loaded FA-CS nanoparticles by NCI-H460 cells

Visual evidence of vincristine loaded folic acid-chitosan nanoparticles (4:25) uptake by the NCI-H460 cells during 45 minutes incubation time at 37 °C was analyzed by fluorescence microscopy using Hoechst 33258 dye. NCI-H460 cells showed diminished fluorescence when grown in RPMI-1640 medium. However, when cells were treated with vincristine loaded folic acid-chitosan conjugated nanoparticles (100 μl), brighter fluorescence was observed at 40× magnifications due to uptake of nanoparticles (Fig. 6). Since, Hoechst 33258 is a blue fluorescent dye used to stain DNA of cells, the fluorescence was observed due to uptake of nanoparticles by cells and their action on DNA. Similarly, Karthikeyan et al. [17] also observed brighter blue fluorescence in NCI-H460 non-small cell lung cancer cells treated with resveratrol loaded gelatin nanoparticles than free resveratrol using Hoechst 33258 dye during 30 minutes incubation time.

3.3.9. Anticancer activity of vincristine loaded FA-CS nanoparticles

Table 4 shows the percent cytotoxicity of blank and vincristine loaded folic acid-chitosan conjugated nanoparticles (5, 10, 15, 20, 25 mg/ml) in NCI-H460 cells. For blank nanoparticles, the lowest cell viability (40.25%) was observed at 20 mg/ml concentration. In comparison, vincristine loaded FA-CS nanoparticles showed lowest cell viability (32.78%) at 10 mg/ml concentration. Hence the inhibitory concentration 50 (IC_{50}) was fixed as 10 mg/ml for blank and 5 mg/ml for vincristine loaded folic acid-chitosan conjugated nanoparticles because at these concentrations, the NCI-H460 non-small cell lung cancer cell line can be used to check intracellular ROS level, changes in mitochondrial transmembrane potential and apoptotic morphological changes without causing damage to cells. For group 1: untreated control cells in RPMI-1640 medium and group 2: untreated control cells in PBS (pH 7.4) with RPMI-1640 medium, almost 100% cell viability was observed, hence not included in the table. Similarly, Wang et al. [31] determined the cytotoxicity of free 5-fluorouracil and 5-fluorouracil loaded hyaluronic acid coated chitosan nanoparticles of different concentrations against A549 cells and HepG2 cells. The results showed that the naked hyaluronic acid-coated chitosan nanoparticles at a concentration (ranging from 0.1 to 1.0 mg/mL) did not inhibit the proliferation of A549 and HepG2 cells, and viability ratios were over 85%. Compared with 5-fluorouracil and 5-fluorouracil-loaded uncoated chitosan nanoparticles, 5-fluorouracil-loaded hyaluronic acid-coated chitosan nanoparticles showed higher cytotoxicity in A549 and HepG2 cells, which was 50% maximal inhibitory concentration (IC_{50}) at 8.0 and 6.7 μg/mL at 48 h, respectively. The cytotoxic effect of hyaluronic acid-coated chitosan nanoparticles was reduced to

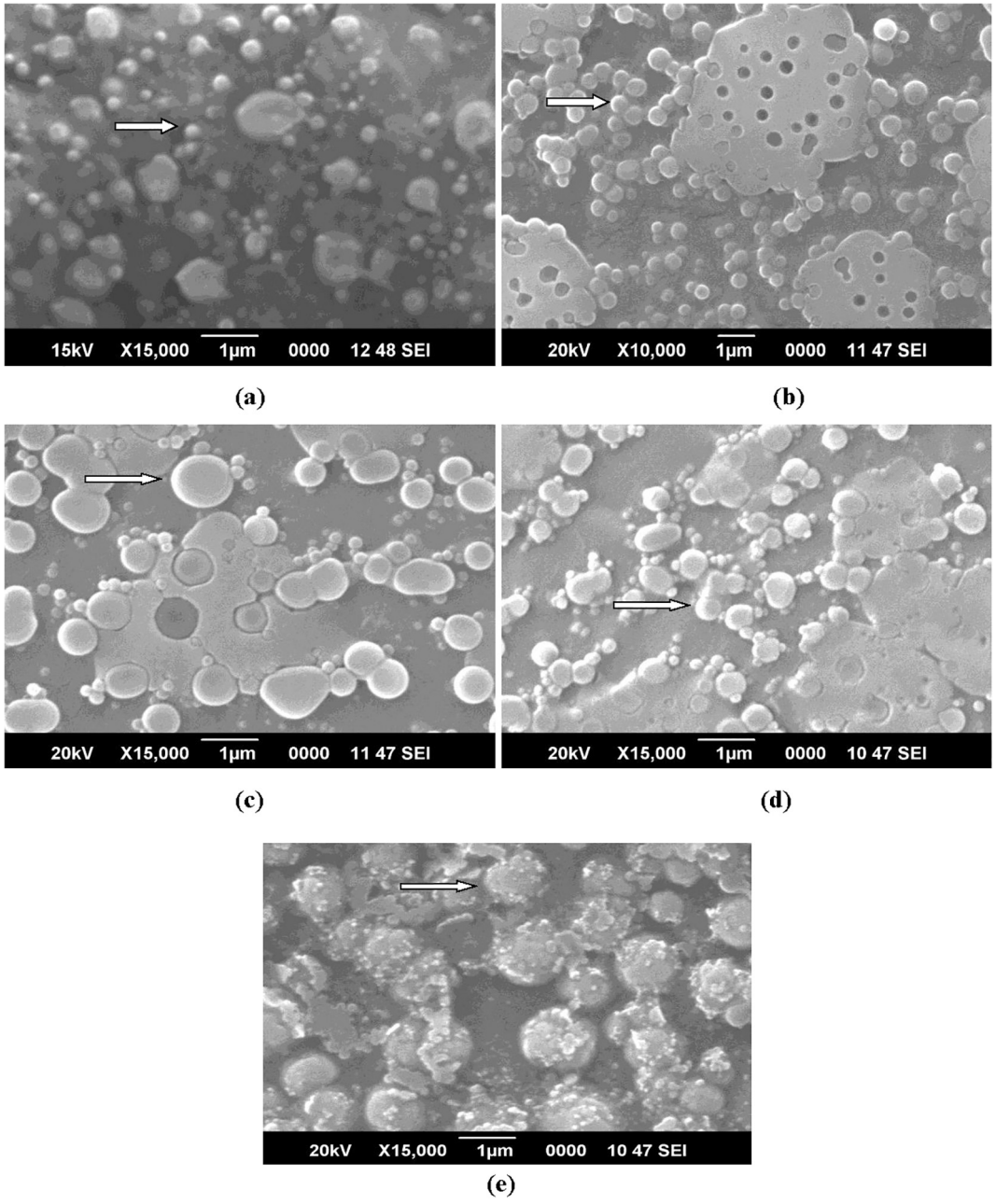

Fig. 3. SEM images of nanoparticles showing spherical shaped (a) blank FA-CS NPs and vincristine loaded FA-CS NPs at different formulations, (b) 1:25, (c) 2:25, (d) 3:25, (e) 4:25.

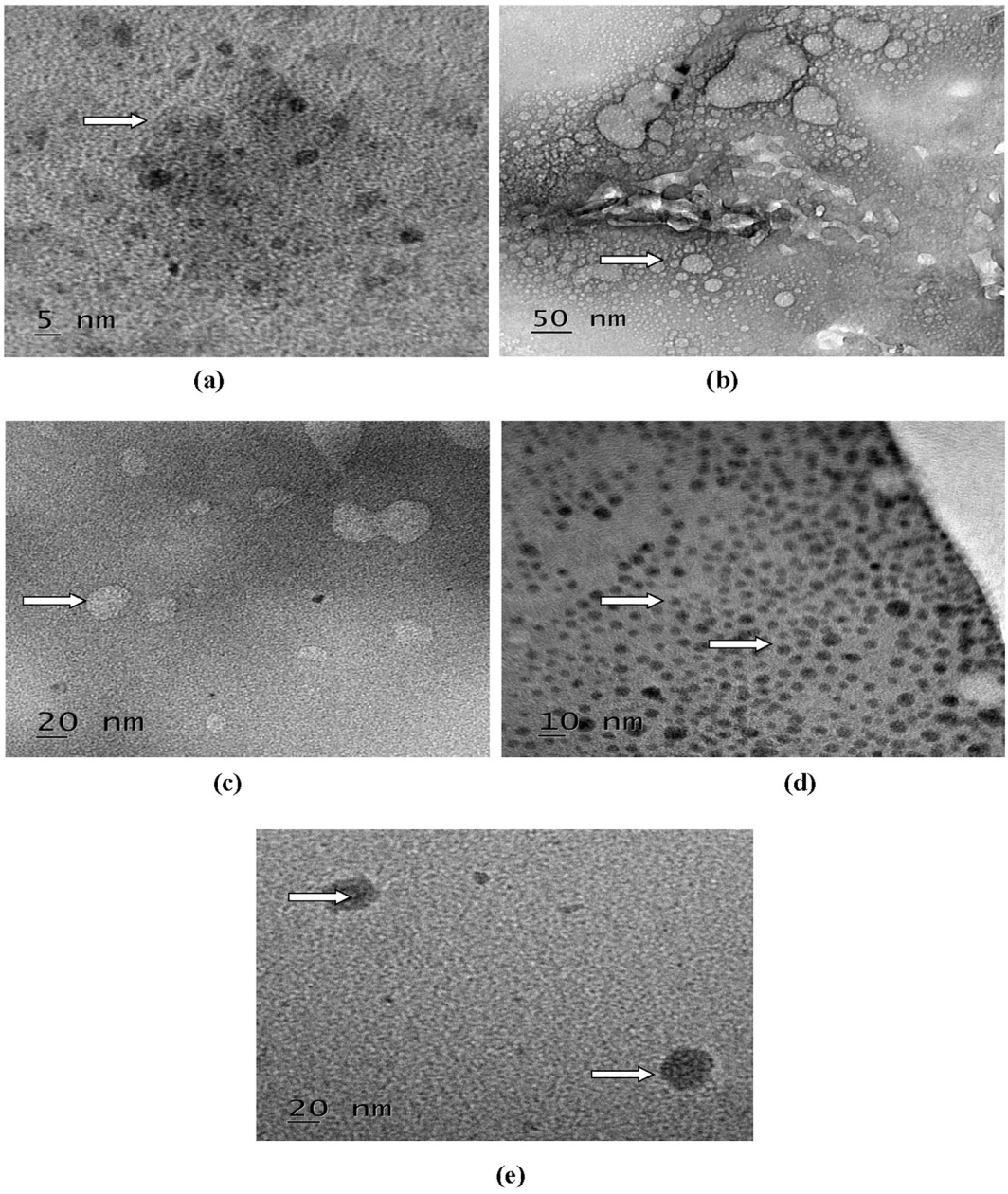

Fig. 4. Transmission electron microphotographs of blank and vincristine loaded FA-CS nanoparticles showing encapsulation of vincristine (arrows) (a) blank and different formulations, (b) 1:25, (c) 2:25, (d) 3:25, (e) 4:25.

13.1 μg/mL at 48 h against A549 cells whereas, addition of free hyaluronic acid had no obvious effects on the HepG2 cells. Anitha et al. [29] studied *in vitro* cytotoxicity of curcumin and curcumin-N,O-carboxymethyl chitosan nanoparticles in a normal (L929), human breast cancer (MCF-7) and prostate cancer cell line (PC-3). L929 cell line treated with N,O-carboxymethyl chitosan nanoparticles showed high cell viability within concentration range of 1–5 mg/ml, whereas reduced cell viability was observed with curcumin and curcumin loaded N,O-carboxymethyl chitosan nanoparticles in the same concentration. However, 80% of the cell viability indicated the non-toxicity of curcumin, N,O-carboxymethyl chitosan nanoparticles and curcumin loaded N,O-carboxymethyl chitosan nanoparticles towards normal cells. For MCF-7 cells, N,O-carboxymethyl chitosan nanoparticles showed no toxicity, whereas curcumin and curcumin N,O-carboxymethyl nanoparticles showed considerable toxicity. Similarly, in PC-3 cells, curcumin-N,O-carboxymethyl chitosan nanoparticles showed toxicity, as a result of which cell viability was reduced to 30% at 5 mg/ml concentration, confirmed its anticancer effects.

3.3.10. Determination of intracellular ROS level

As shown in (Fig. 7i), weak ROS generation was observed in the untreated NCI-H460 cells. In contrast, blank nanoparticles showed significant ROS production and a further enhanced ROS generation, was found in vincristine loaded folic acid-chitosan conjugated nanoparticles (Fig. 7i). Similarly, Hou et al. [32] observed ROS level in human lung carcinoma (A549) and cervical cancer cell line (HeLa) treated with triphenyl phosphine-functionalized chitosan nanoparticles through targeted delivery of doxorubicin to mitochondria. The results demonstrated that ROS levels in A549 and HeLa cells exposed to free doxorubicin showed a certain enhancement and were increased to 120.5% in 24 h and 130.4% after 48 h in

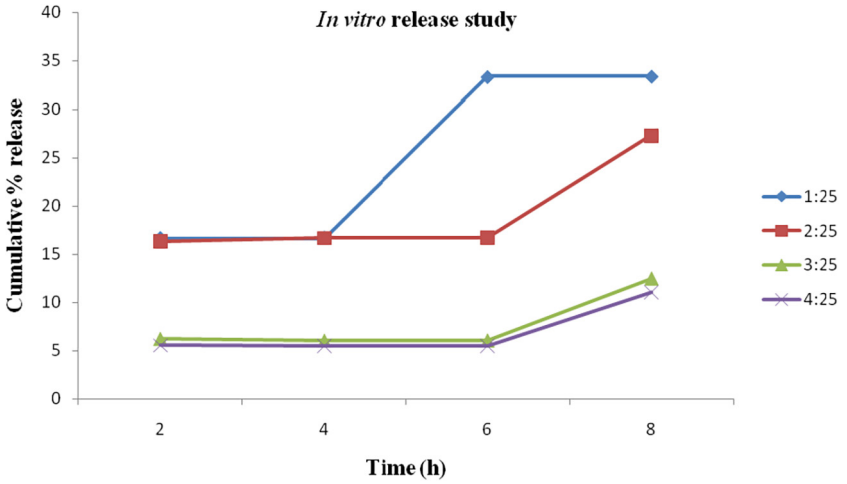

Fig. 5. Cumulative release (%) behavior of vincristine from folic acid-chitosan conjugated nanoparticles for different formulations (1:25, 2:25, 3:25, 4:25) showing slow and sustained release in phosphate buffered saline (pH 6.7).

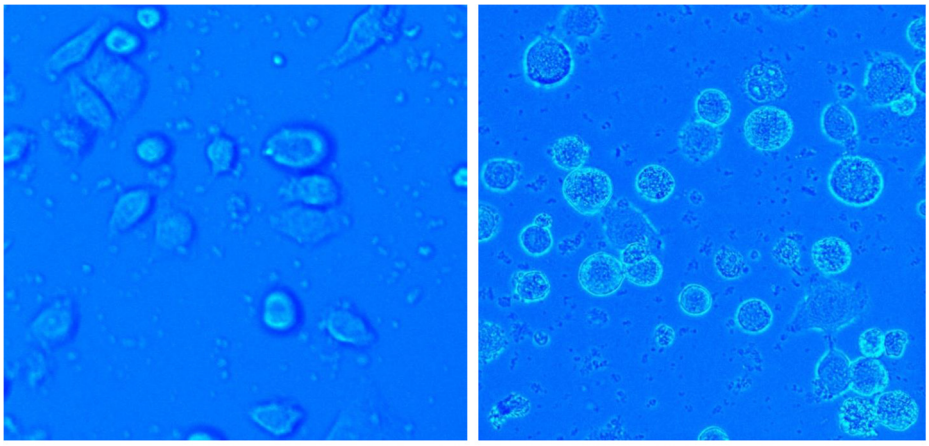

Fig. 6. Cellular uptake of nanoparticles in NCI-H460 cells 40× (a) control, (b) enhanced fluorescence with vincristine loaded folic acid-chitosan conjugated nanoparticles.

A549 cells in comparison with 130.4% in 24 h and 136.7% after 48 h in HeLa cells. In the same way, doxorubicin-loaded triphenyl phosphine-functionalized chitosan nanoparticles also triggered ROS levels at 168.4% in 24 h and 180.4% after 48 h in A549 cells, and 150.1% in 24 h and 166.5% after 48 h in HeLa cells.

3.3.11. Determination of changes in mitochondrial transmembrane potential

NCI-H460 cells treated with blank FA-CS nanoparticles and untreated control cells (Fig. 7ii) showed blue fluorescence due to accumulation of Rh-123 dye. However, no Rh-123 accumulation was found in vincristine loaded folic acid-chitosan conjugated nanoparticles treated cells (Fig. 7ii). Hence, mitochondrial membrane potential has been found to be reduced in the cells treated with vincristine loaded FA-CS nanoparticles. Karthikeyan et al. [17] observed reduced mitochondrial membrane potential in NCI-H460 cells treated with resveratrol-loaded gelatin nanoparticles as compared to resveratrol. They found accumulation of Rh-123 dye in the control group whereas, resveratrol-loaded gelatin nanoparticles treated cells showed decreased membrane potential.

Table 4
Cell viability (%) of blank and vincristine loaded FA-CS nanoparticles at different concentrations.

S. No.	Concentration (mg/ml)	Cell viability (%)	
		Blank FA-CS NPs	Vincristine loaded FA-CS NPs
1.	5	87.14	46.47
2.	10	71.49	32.78
3.	15	52.89	43.15
4.	20	40.25	38.17
5.	25	47.25	36.51

3.3.12. Determination of apoptotic morphological changes

Very less morphological changes associated with acridine orange and ethidium bromide were observed in control and NCI-H460 cells treated with blank FA-CS nanoparticles (Fig. 7iii). When NCI-H460 cells were treated with vincristine loaded folic acid-chitosan conjugated nanoparticles (5 mg/ml, 50 μl), apoptotic features with differential staining of acridine orange and ethidium bromide were observed. This showed that vincristine loaded folic acid chitosan conjugated nanoparticles were more effective than blank nanoparticles. Finally, vincristine loaded folic acid-chitosan conjugated nanoparticles showed 75% of apoptotic cells, whereas for blank 31% cells were observed with apoptosis. Karthikeyan et al. [17] observed apoptotic features with condensed or frag-

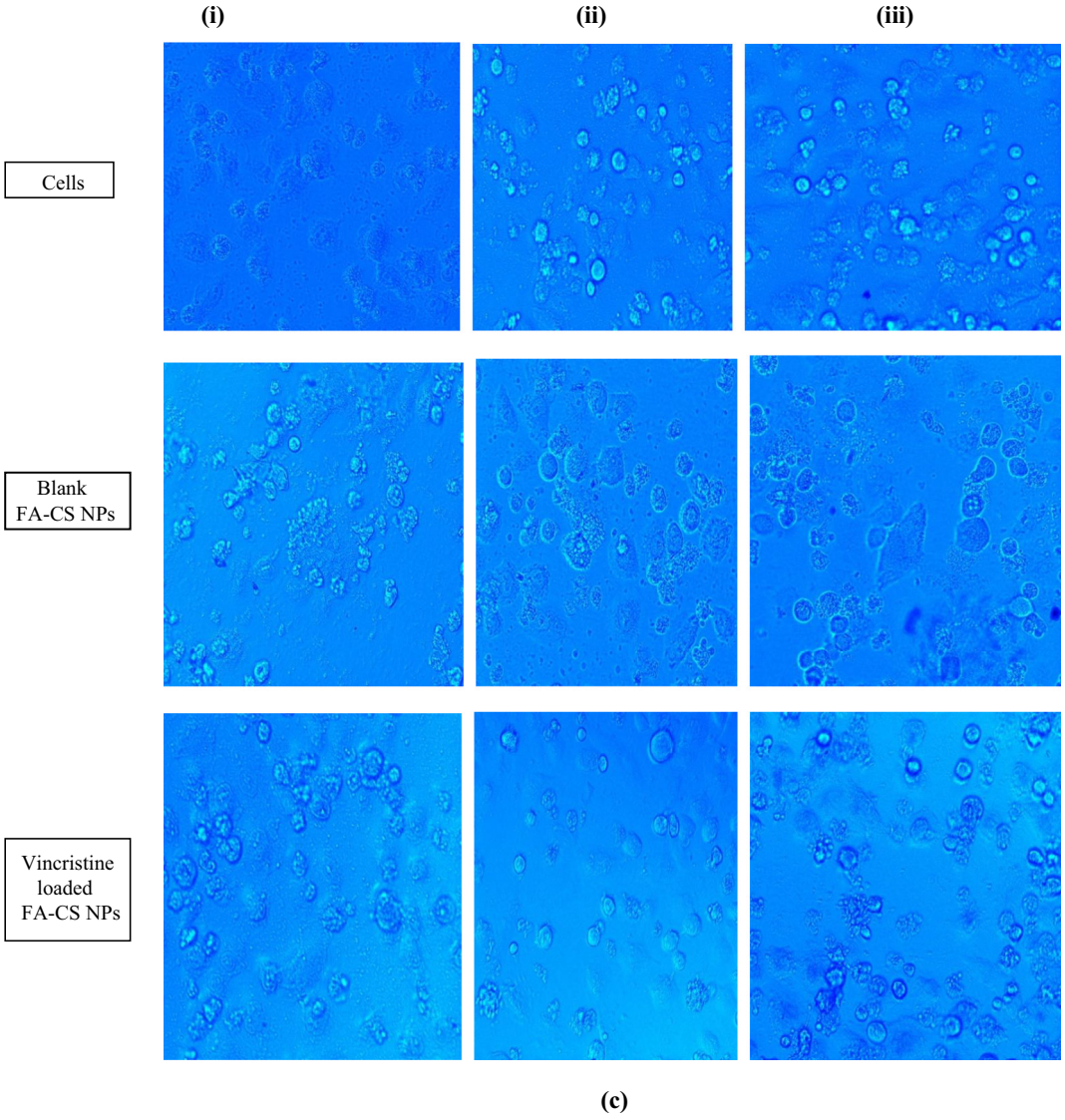

Fig. 7. Fluorescent micrographs showing effect of nanoparticles in NCI-H460 cells (i) intracellular ROS level, (ii) mitochondrial transmembrane potential, (iii) apoptotic morphological changes.

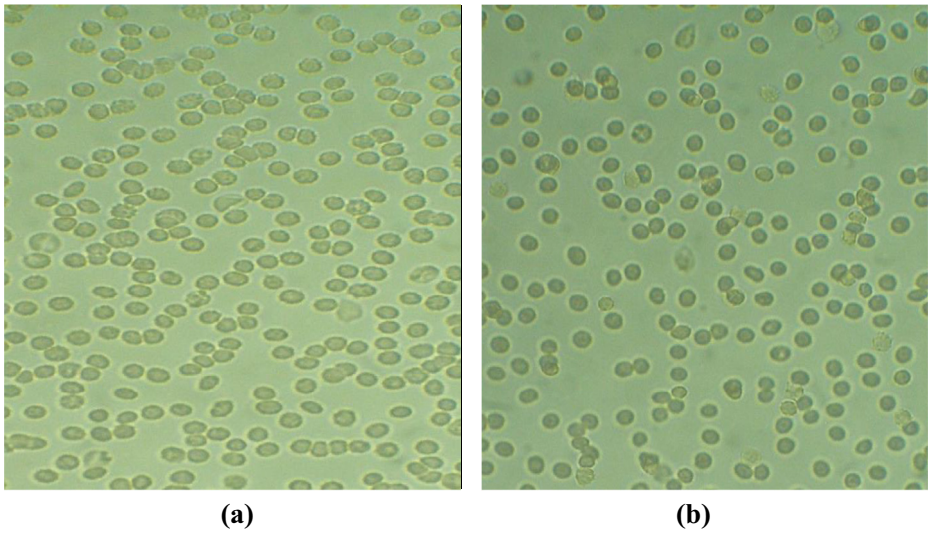

Fig. 8. Light microphotographs of erythrocytes aggregation (a) control, (b) vincristine loaded folic acid-chitosan conjugated nanoparticles.

mented chromatin, indicative of apoptosis in resveratrol and resveratrol-loaded gelatin nanoparticles treated NCI-H460 cells. Resveratrol-loaded gelatin nanoparticles treated NCI-H460 cells showed 98% apoptosis, whereas free resveratrol treatment showed only 42% apoptotic cells. Similarly, Panwar et al. [28] determined apoptotic morphological changes of ferulic acid-loaded chitosan nanoparticles against human cervical cancer cell line (ME-180) with acridine orange (AO) and ethidiumbromide (EtBr) staining. Cells treated with ferulic acid chitosan-tripolyphosphate pentasodium nanoparticles (40 μM) for 24 h displayed morphological characteristics such as higher cell shrinkage, cytoplasmic condensation, and irregularity in shape, suggested that ferulic acid-loaded chitosan nanoparticles could induce apoptotic cell death in ME-180 cells. The morphology and growth of cancer cells cultured on unloaded chitosan-tripolyphosphate pentasodium nanoparticles were negligibly affected as compared to control.

4. Erythrocyte aggregation assay

As shown in Fig. 8(a), fresh erythrocytes were spherical in shape. After treatment with vincristine loaded folic acid-chitosan conjugated nanoparticles (400 μl, 4:25 formulation) in phosphate buffered saline (PBS, pH 7.4) for 1 h at 37 °C, no aggregation of erythrocytes was reported as shown in Fig. 8(b). This showed that 4:25 formulation was safe for erythrocytes. Similarly, Karthikeyan et al. [17] also observed no aggregation of erythrocytes when treated with resveratrol-loaded gelatin nanoparticles.

5. Conclusion

In this study, vincristine was loaded in folic acid-chitosan conjugated nanoparticles in different formulations i.e. 1:25, 2:25, 3:25, 4:25 at pH 5. Maximum encapsulation efficiency (%) and loading capacity (%) was observed for 4:25 formulation i.e. 95 ± 0.35 and 48.65 ± 0.47, respectively. Scanning electron microscopy showed spherical structure with rough surfaced nanoparticles. Fourier transform infrared spectroscopy (FTIR) and Transmission electron microscopy (TEM) confirmed encapsulation of vincristine in nanoparticles. Attachment of folic acid, size of nanoparticles below 200 nm in all formulations with positive zeta potential favored targeted delivery of vincristine to cancer cells. Anticancer activity of vincristine loaded folic acid chitosan nanoparticles in 4:25 formulation was checked against non-small cell lung cancer cell line (NCI-H460). MTT assay showed greater cytotoxicity of vincristine loaded folic acid chitosan conjugated nanoparticles as compared to blank. Enhanced ROS generation, decreased mitochondrial transmembrane potential and apoptotic morphological changes associated with NCI-H460 cells showed effectiveness of vincristine loaded folic acid-chitosan conjugated nanoparticles in the treatment of NCI-H460 cells. No aggregation of erythrocytes was reported when treated with vincristine loaded folic acid-chitosan conjugated nanoparticles. Hence vincristine loaded folic acid-chitosan conjugated nanoparticles in 4:25 formulation can be used for treatment of NCI-H460 cells.

Acknowledgements

The authors acknowledge Central Instrumentation Laboratory and Sophisticated Analytical Instrumentation Facility, Panjab University, Chandigarh for help in FTIR and XRD analyses, respectively. Authors are thankful to Sophisticated Test & Instrumentation Centre, Cochin University of Science and Technology, Cochin for help in SEM and TEM analysis. The authors also acknowledge Prof. Tibor Hianik and Zuzana Garaiova, Department of Nuclear Physics and Biophysics, Faculty of Mathematics, Physics and Informatics, Comenius University, Bratislava, Slovak Republic for help in average size, polydispersity index, zeta potential measurements. Naresh Kumar gratefully acknowledges Slovak Academic Information Agency, Bratislava for awarding National Scholarship under National Scholarship Programme approved by the Government of the Slovak Republic to carry out some part of research work at Slovakia and University Research Scholarship from Chaudhary Devi Lal University, Sirsa, Haryana.

References

[1] Ferlay J, Soerjomataram I, Ervik M, Dikshit R, Eser S, Mathers C, et al. GLOBOCAN 2012 v1.0, Cancer Incidence and Mortality Worldwide: IARC CancerBase No. 11. Lyon, France: International Agency for Research on Cancer; 2012.
[2] Travis WD, Travis LB, Devesa SS. Lung cancer. Cancer 1995;75:191–202.
[3] Costa G, Hreshchyshyn MM, Holland JF. Initial clinical studies with vincristine. Cancer Chemother Rep 1962;24:39–44.
[4] Johnson IS, Armstrong JG, Gorman M, Burnett Jr JP. The vinca alkaloids: a new class of oncolytic agents. Cancer Res 1963;23:1390–427.
[5] Vincristine sulfate. The American Society of Health-System Pharmacists [retrieved 11.07.17].
[6] Ravina E. The evolution of drug discovery: from traditional medicines to modern drugs. 1 Aufl Ed. Weinheim; 2011, p. 157–15.
[7] Kumar MR, Muzzarelli RA, Muzzarelli C, Sashiwa H, Domb A. Chitosan chemistry and pharmaceutical perspectives. Chem Rev 2004;104:6017–84.
[8] Ilium L. Chitosan and its use as a pharmaceutical excipient. Pharm Res 1998;15:1326–31.
[9] Felt O, Buri P, Gurny R. Chitosan: a unique polysaccharide for drug delivery. Drug Dev Ind Pharm 1998;24:979–93.
[10] Kean T, Thanou M. Chitin and chitosan-sources, production and medical applications. In: Williams PA, Arshady R, editors. Desk reference of natural polymers, their sources, chemistry and applications. London: Kentus Books; 2009. p. 327–61.
[11] Mourya VK, Inamdar NN. Chitosan-modifications and applications: opportunities galore. React Funct Polym 2008;68:1013–51.
[12] Subramanian A, Rau AV, Kaligotla H. Surface modification of chitosan for selective surface-protein interaction. Carbohydr Polym 2006;66:321–32.
[13] Byrne JD, Betancourt T, Brannon-Peppas L. Active targeting schemes for nanoparticle systems in cancer therapeutics. Adv Drug Deliv Rev 2008;60:1615–26.
[14] Salar RK, Kumar N. Synthesis and characterization of vincristine loaded folic acid–chitosan conjugated nanoparticles. Res Eff Technol 2016;2:199–214.
[15] Calvo P, Remunan Lopez C, VilaJato JL, Alonso MJ. Novel hydrophilic chitosan-polyethylene oxide nanoparticles as protein carriers. J Appl Polym Sci 1997;63:125–32.
[16] Mosmann T. Rapid colorimetric assay for cellular growth and survival: application to proliferation and cytotoxicity assays. J Immunol Methods 1983;65:55–63.
[17] Karthikeyan S, Rajendra Prasad N, Ganamani A, Balamurugan E. Anticancer activity of resveratrol-loaded gelatin nanoparticles on NCI-H460 non-small cell lung cancer cells. Biomed Prev Nutr 2013;3:64–73.
[18] Ji J, Wu D, Liu L, Chen J, Xu Y. Preparation, characterization, and *in vitro* release of folic acid-conjugated chitosan nanoparticles loaded with methotrexate for targeted delivery. Polym Bull 2012;68:1707–20.
[19] Wang W, Tong C, Liu X, Li T, Liu B, Xiong W. Preparation and functional characterization of tumor-targeted folic acid-chitosan conjugated nanoparticles loaded with mitoxantrone. J Cent South Univ 2015;22:3311–7.
[20] Naghibi Beidokhti HR, Ghaffarzadegan R, Mirzakhanlouei S, Ghazizadeh L, Dorkoosh FA. Preparation, characterization, and optimization of folic acid-chitosan-methotrexate core-shell nanoparticles by Box-Behnken design for tumor-targeted drug delivery. AAPS PharmSciTech 2017;18:115–29.
[21] Selvi Gunel N, Ozel B, Kipcak S, Aktan C, Akgun C, Ak G, et al. Synthesis of methotrexate loaded chitosan nanoparticles and *in vitro* evaluation of the potential in treatment of prostate cancer. Anticancer Agents Med Chem 2016;16:1038–42.
[22] Maeda H, Wu J, Sawa T, Matsumura Y, Hori K. Tumor vascular permeability and the EPR effect in macromolecular therapeutics: a review. J Control Release 2000;65:271–84.
[23] Owens IIIrd DE, Peppas NA. Opsonization, biodistribution, and pharmacokinetics of polymeric nanoparticles. Int J Pharm 2006;307:93–102.
[24] Sun L, Chen Y, Zhou Y, Guo D, Fan Y, Guo F, et al. Preparation of 5-fluorouracil-loaded chitosan nanoparticles and study of the sustained release *in vitro* and *in vivo*. Asian J Pharm Sci 2017;12:418–23.
[25] Xu S, Xu Q, Zhou J, Wang J, Zhang N, Zhang L. Preparation and characterization of folate-chitosan-gemcitabine core-shell nanoparticles for potential tumor-targeted drug delivery. J Nanosci Nanotechnol 2013;13:129–38.
[26] Tsai ML, Chen R-H, Bai S-W, Chen W-Y. The storage stability of chitosan/tripolyphosphate nanoparticles in a phosphate buffer. Carbohydr Polym 2014;84:756–61.
[27] Xu YM, Du YM. Effect of molecular structure of chitosan on protein delivery properties of chitosan nanoparticles. Int J Pharm 2003;250:215–26.

[28] Panwar R, Sharma AK, Kaloti M, Dutt D, Pruthi V. Characterization and anticancer potential of ferulic acid-loaded chitosan nanoparticles against ME-180 human cervical cancer cell lines. Appl Nanosci 2016;6:803–13.
[29] Anitha A, Maya S, Deepa N, Chennazhi KP, Nair SV, Jayakumar R. Curcumin-loaded N,O-carboxymethyl chitosan nanoparticles for cancer drug delivery. J Biomater Sci Polym Ed 2013;23:1381–400.
[30] Mehrotra A, Nagarwal RC, Pandit JK. Fabrication of lomustine loaded chitosan nanoparticles by spray drying and *in vitro* cytostatic activity on human lung cancer cell line L132. J Nanomed Nanotechnol 2010;1:103. doi: https://doi.org/10.4172/2157-7439.1000103.
[31] Wang T, Hou J, Su C, Zhao L, Shi Y. Hyaluronic acid-coated chitosan nanoparticles induce ROS-mediated tumor cell apoptosis and enhance antitumor efficiency by targeted drug delivery via CD44. J Nanobiotechnol 2017;15:7. doi: https://doi.org/10.1186/s12951-016-0245-2.
[32] Hou J, Yu X, Shen Y, Shi Y, Su C, Zhao L. Triphenyl phosphine-functionalized chitosan nanoparticles enhanced antitumor efficiency through targeted delivery of doxorubicin to mitochondria. Nanoscale Res Lett 2017;12:158. doi: https://doi.org/10.1186/s11671-017-1931-1.